Electronic Supplementary Material (ESI) for Journal of Materials Chemistry A.

Supplementary Information

Engineering anisotropic structures of thermally insulating aerogels with high solar reflectance for energy-efficient cooling applications

Eunyoung Kim,[1]† Kit-Ying Chan,[2]† Jie Yang,[1] Harun Venkatesan,[1] Miracle Hope Adegun,[1] Heng Zhang,[1] Jeng-Hun Lee,[1] Xi Shen,[2,3]* Jang-Kyo Kim[1,4]*

[1] Department of Mechanical and Aerospace Engineering, The Hong Kong University of Science and Technology, Clearwater Bay, Kowloon, Hong Kong

[2] Department of Aeronautical and Aviation Engineering, The Hong Kong Polytechnic University, Hung Hom, Kowloon, Hong Kong

[3] The Research Institute for Sports Science and Technology, The Hong Kong Polytechnic University, Hung Hom, Kowloon, Hong Kong

[4] School of Mechanical and Manufacturing Engineering, The University of New South Wales, Sydney, NSW 2052, Australia

†Eunyoung Kim and Kit-Ying Chan share equal first authorship

*Corresponding authors: Xi Shen (xi.shen@polyu.edu.hk); Jang-Kyo Kim (mejkkim@ust.hk)

S1. Characterization of BNNS and BNNS/WPU composite aerogels

The morphologies and chemical structures of exfoliated BNNS from bulk *h*-BN were characterized (Supplementary Figure 1). The SEM image shows that the lateral size of BNNS is in the range of several hundred nanometers to 5 μm (Supplementary Figure 1a). The AFM profile presents an ultrathin thickness of BNNS ranging from 3 to 7 nm (Supplementary Figure 1b-c). The crystalline structures of bulk *h*-BN and BNNS were studied by XRD (Supplementary Figure 1d). Both materials exhibited prominent peaks of the (002), (100), (101), (102) and (004) planes at 26.7º, 41.7º, 44.0º, 50.5º and 54.3º, respectively, confirming an intact crystalline structure of *h*-BN after the chemical exfoliation to form BNNS.[1, 2] The XPS survey spectra (Supplementary Fig. 1e) of both WPU and BNNS/WPU aerogels showed peaks at 285, 400 and 533 eV corresponding to C1*s*, N1*s* and O1*s*, respectively. An additional B1*s* peak was detected at 190.2 eV for the BNNS/WPU aerogel because of the presence of BNNS. The deconvoluted B1*s* spectrum (Supplementary Fig. 1f) presented two major peaks of B-O and B-N bonds at 191.2 eV and 190.5 eV, respectively. The presence of B-O bonds indicates the formation of pendant hydroxyl groups on BN skeletons due to hydrolysis taking place during exfoliation.[3-5] This would facilitate the formation of hydrogen bonds between the hydroxyl groups on BNNS and the ether or carboxyl groups in the WPU chains, promoting interfacial interaction between them.[6, 7]

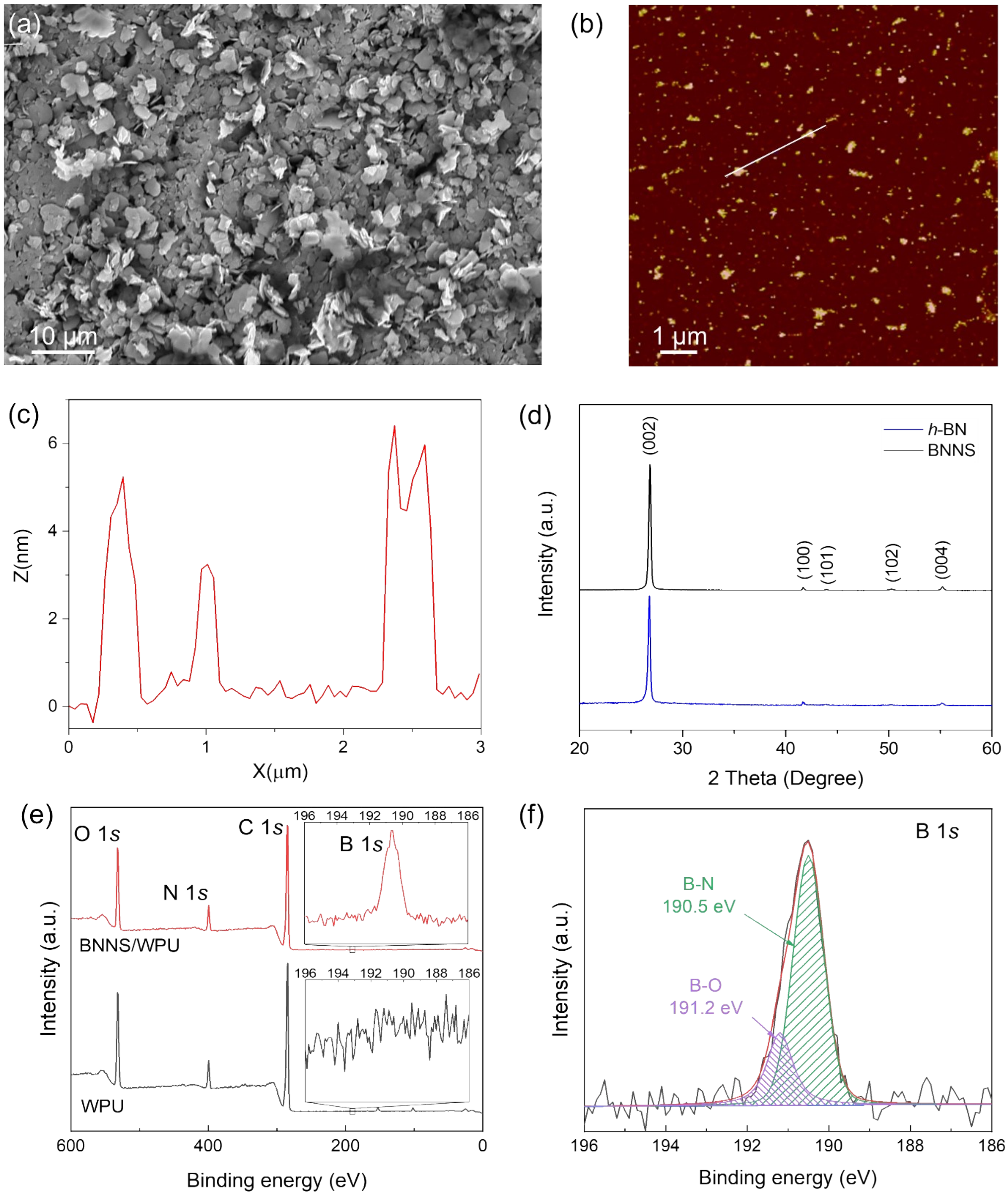

Supplementary Figure 1. Characterization of *h*-BN and BNNS. (a) SEM, (b) AFM images, and (c) the thickness profile obtained from AFM showing the lateral size and thickness of BNNS. (d) XRD patterns of bulk *h*-BN and BNNS. (e) XPS spectra of WPU and BNNS/WPU aerogels. (f) High-resolution B1*s* spectrum of BNNS/WPU aerogel.

S2. Thermal response of BNNS/WPU composite aerogels

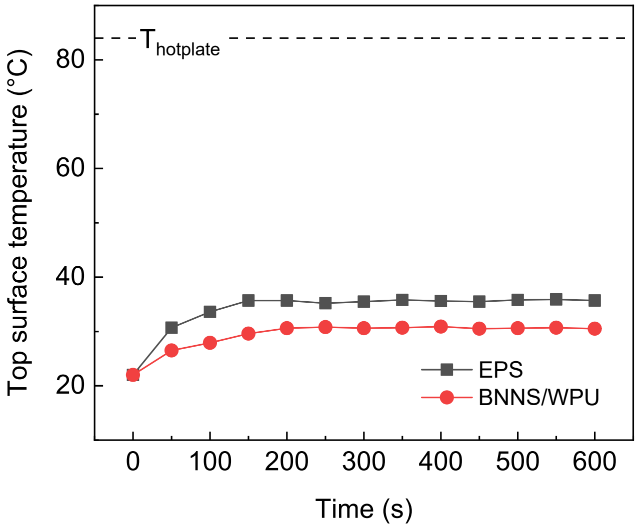

Supplementary Figure 2. Top surface temperatures of the BNNS/WPU aerogels and commercial EPS foam (k = 30.5 mW/ m K) measured using a thermal camera.

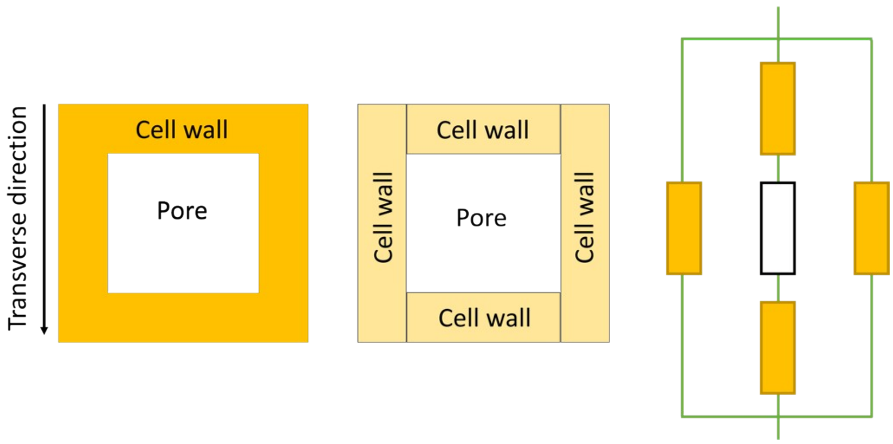

Supplementary Figure 3. Total thermal resistor network of heat flux in the transverse direction.

The k of the BNNS/WPU composite cell wall in the transverse and alignment directions, *i.e.*, k_{wall}^{x} and k_{wall}^{y}, are estimated using the effective medium approximation according to previous studies:[8, 9]

$$k_{wall}^{y} = k_m \frac{2 + f\left[\beta_y(1 - L_y)\left(1 + \langle\cos^2\theta\rangle\right) + \beta_x(1 - L_x)\left(1 - \langle\cos^2\theta\rangle\right)\right]}{2 - f\left[\beta_y L_y\left(1 + \langle\cos^2\theta\rangle\right) + \beta_x L_x\left(1 - \langle\cos^2\theta\rangle\right)\right]} \quad \text{(S1)}$$

$$k_{wall}^{x} = k_m \frac{1 + f\left[\beta_y(1 - L_y)(1 - \langle \cos^2\theta \rangle) + \beta_x(1 - L_x)\langle \cos^2\theta \rangle\right]}{1 - f\left[\beta_y L_y(1 - \langle \cos^2\theta \rangle) + \beta_x L_x \langle \cos^2\theta \rangle\right]} \quad \text{(S2)}$$

$$\beta_i = \frac{k_i^c - k_m}{k_m + L_i(k_i^c - k_m)} \quad \text{(S3)}$$

$$L_y = L_z = \frac{p^2}{2(p^2 - 1)} + \frac{p}{2(1 - p^2)^{3/2}} \cos^{-1} p, \text{ for } p = \frac{a_3}{a_1} < 1 \quad \text{(S4)}$$

$$L_x = 1 - 2L_y \quad \text{(S5)}$$

$$k_i^c = \frac{k_p}{1 + \frac{\gamma L_i k_p}{k_m}} \quad \text{(S6)}$$

$$\gamma = (1 + 2p)\alpha, \text{ for } p \leq 1 \quad \text{(S7)}$$

$$\alpha = \frac{R_{BD}}{K_m h} \quad \text{(S8)}$$

where f is the volume fraction of BNNS, k_m is the k of WPU (0.21 W/mK), k_p is the k of BNNS (600 W/mK),[10] $\langle \cos^2\theta \rangle$ equals to 1 for parallel flat plate inclusions oriented perpendicular to the X_3 axis, and equal to $\frac{1}{3}$ for completely random plates, α is a dimensionless parameter, R_{BD} is the Kapitza interfacial thermal resistance between BNNS and polymer matrix (7.6×10^{-9} m^2 K/W),[11] and h is the thickness of BNNS.

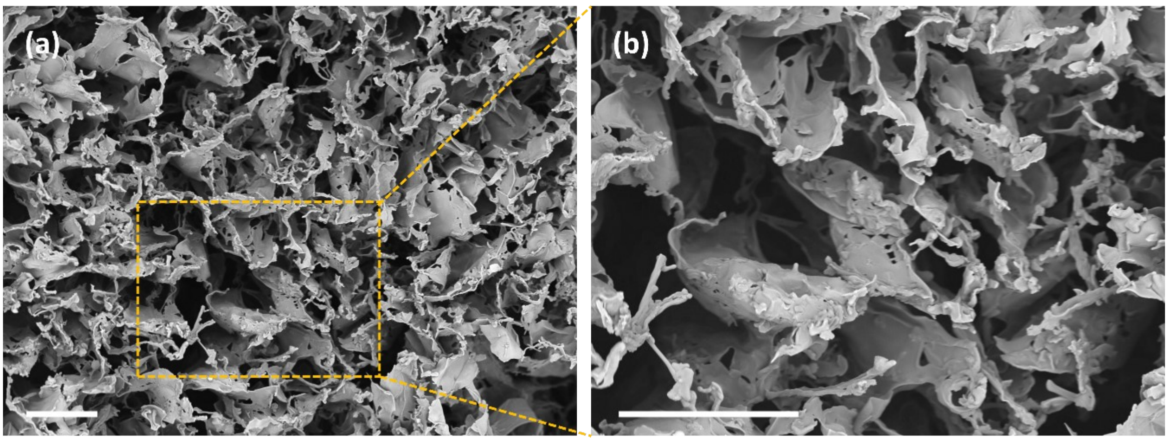

Supplementary Figure 4. SEM images showing the presence of holes in the cell walls. The scale bars are 100 μm.

S3. Outdoor test of BNNS/WPU composite aerogels

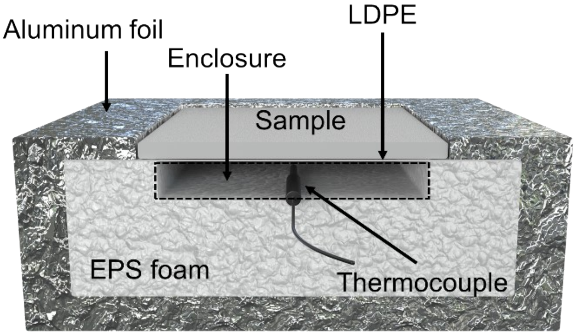

Supplementary Figure 5. Schematical illustration of set-up for outdoor test.

Supplementary Table 1. Physical properties of WPU and WPU/BNNS aerogels fabricated at different freezing temperatures and BNNS contents.

Freezing temperature (°C)	BNNS loading (wt%)	Density (mg/cm^3)	Porosity (%)
-20	0	36.7 ± 2.0	96.4
	10	35.5 ± 1.4	96.7
-50	0	28.6 ± 2.3	97.2
	10	27.1 ± 0.8	97.5
-196	0	25.5 ± 0.2	97.5
	10	20.2 ±0.6	98.1

Supplementary Table 2. Comparison of thermal and optical properties of the current BNNS/WPU aerogel with other structures reported in the literature.

Materials	k_{trans} (for anisotropic structure) or k (for isotropic structure) (mW/m K)	Solar reflectance (%)	Reference
BNNS/PVA aerogel	23.5	93.8	12
PE aerogel	28	92.2	13
PDMS/PE aerogel	32	96	14
Superhydrophobic cellulose aerogel	28	93	15
CNC aerogel	26	96	16
Hollow microfibers cooler	14	94	17
Nanowood	30	95	18
TiO_2/Silica aerogel nanocomposite	29	90	19
BNNS/WPU aerogel	**16.2**	**97**	**This work**

Supplementary references

1. X. Hou, M. Wang, L. Fu, Y. Chen, N. Jiang, C.-T. Lin, Z. Wang and J. Yu, *Nanoscale*, 2018, **10**, 13004-13010.
2. D. Fan, J. Feng, J. Liu, T. Gao, Z. Ye, M. Chen and X. Lv, *Ceram. Int.*, 2016, **42**, 7155-7163.
3. B. Zhang, Q. Wu, H. Yu, C. Bulin, H. Sun, R. Li, X. Ge and R. Xing, *Nanoscale Res. Lett.*, 2017, **12**, 1-7.
4. W. Wang, S. J. Chen, F. B. De Souza, B. Wu and W. H. Duan, *Nanoscale*, 2018, **10**, 1004-1014.
5. Y. Shi, C. Hamsen, X. Jia, K. K. Kim, A. Reina, M. Hofmann, A. L. Hsu, K. Zhang, H. Li and Z.-Y. Juang, *Nano Lett.*, 2010, **10**, 4134-4139.
6. F. Liu, R. Han, S. Naficy, G. Casillas, X. Sun and Z. Huang, *ACS Applied Nano Materials*, 2021, **4**, 7988-7994.
7. X. Li, P. Bandyopadhyay, T. Kshetri, N. H. Kim and J. H. Lee, *J. Mater. Chem. A*, 2018, **6**, 21501-21515.
8. C.-W. Nan, R. Birringer, D. R. Clarke and H. Gleiter, *J. Appl. Phys.*, 1997, **81**, 6692-6699.
9. X. Shen, Z. Wang, Y. Wu, X. Liu, Y.-B. He and J.-K. Kim, *Nano Lett.*, 2016, **16**, 3585-3593.
10. S. Yu, X. Shen and J.-K. Kim, *Mater. Horiz.*, 2021, **8**, 3009-3042.

11. Z.-G. Wang, W. Liu, Y.-H. Liu, Y. Ren, Y.-P. Li, L. Zhou, J.-Z. Xu, J. Lei and Z.-M. Li, *Compos. B Eng.*, 2020, **180**, 107569.
12. J. Yang, K.-Y. Chan, H. Venkatesan, E. Kim, M. H. Adegun, J.-H. Lee, X. Shen and J. K. Kim, *Nano-Micro Lett.*, 2022, **14**, 1-16.
13. A. Leroy, B. Bhatia, C. C. Kelsall, A. Castillejo-Cuberos, M. Di Capua H, L. Zhao, L. Zhang, A. Guzman and E. Wang, *Sci. Adv.*, 2019, **5**, eaat9480.
14. M. Yang, W. Zou, J. Guo, Z. Qian, H. Luo, S. Yang, N. Zhao, L. Pattelli, J. Xu and D. S. Wiersma, *ACS Appl. Mater. Interfaces*, 2020, **12**, 25286-25293.
15. X. Yue, H. Wu, T. Zhang, D. Yang and F. Qiu, *Energy*, 2022, **245**, 123287.
16. C. Cai, Z. Wei, C. Ding, B. Sun, W. Chen, C. Gerhard, E. Nimerovsky, Y. Fu and K. Zhang, *Nano Lett.*, 2022, **22**, 4106-4114.
17. H. Zhong, Y. Li, P. Zhang, S. Gao, B. Liu, Y. Wang, T. Meng, Y. Zhou, H. Hou and C. Xue, *ACS Nano*, 2021, **15**, 10076-10083.
18. Z.-L. Yu, N. Yang, L.-C. Zhou, Z.-Y. Ma, Y.-B. Zhu, Y.-Y. Lu, B. Qin, W.-Y. Xing, T. Ma and S.-C. Li, *Sci. Adv.*, 2018, **4**, eaat7223.
19. L. An, D. Petit, M. Di Luigi, A. Sheng, Y. Huang, Y. Hu, Z. Li and S. Ren, *ACS Appl. Nano Mater.*, 2021, **4**, 6357-6363.